CONF-921110--43

# CHAOTIC VIBRATIONS OF TUBES WITH NONLINEAR SUPPORTS IN CROSSFLOW

by

ANL/CP--75489

DE93 004247

Y. Cai and S. S. Chen

Materials and Components Technology Division
Argonne National Laboratory
9700 South Cass Avenue, Argonne, Illinois 60439





To be submitted for presentation at the 1992 ASME/JSME/IMechE/CSME/IAHR Int'l Symposium on Flow-Induced Vibration and Noise, November 8-13, 1992, Anaheim, CA

*Work supported by the US Department of Energy, Office of Basic Energy Sciences

## ABSTRACT

By means of the unsteady flow theory and a bilinear mathematical model, a theoretical study is presented for chaotic vibrations associated with the fluidelastic instability of nonlinearly supported tubes in a crossflow. A series of effective tools, including phase portraits, power spectral density, Poincaré maps, Lyapunov exponent, fractal dimension, and bifurcation diagrams, are utilized to distinguish periodic and chaotic motions when the tubes vibrate in the instability region. The results show periodic and chaotic motions in the region corresponding to the fluid damping controlled instability. Nonlinear supports, with symmetric or asymmetric gaps, significantly affect the distributions of periodic, quasiperiodic and chaotic motions of the tube with various flow velocity in the instability region of the TSP(tube-support-plate)-inactive mode.

## NOMENCLATURE

| | |
|---|---|
| $a_{in}, \dot{a}_{in}$ | Generalized tube displacement and velocity for Model i |
| C | Correlation function |
| D | Tube diameter |
| $d_G$ | Correlation dimension |
| E | Young's modulus |
| $e_1$, $e_2$ | Tube–support gaps |
| f | Oscillation frequency |
| $f_n$ | Natural frequency of n-th mode |
| I | Moment of inertia of tube cross section |
| $K_c$ | Equivalent stiffness |
| $k_{in}$ | Eigenvalues for tube vibration for Model i |
| $\ell$ | Tube length |
| m | Mass per unit length |
| N | Number of total points in Poincaré maps |
| n | Number of modes |
| P | Pitch |
| R | Radius of tube |
| r | Sphere length |
| t | Time |
| $t_s$ | Time when tube strikes TSP |
| $t_d$ | Time when tube leaves TSP |
| $U_m$ | Mean flow velocity |

| | |
|---|---|
| $U_r$ | Reduced flow velocity (= $U_m/fD$ or $U/fD$) |
| $u_i$, $\dot{u}_j$ | Displacement and velocity |
| $x_i$ | Points in phase space of Poincaré map |
| $\alpha_{in}$ | Added–mass coefficients of n–th mode for Model i |
| $\alpha_{in}^d$ | Fluid damping coefficients of n–th mode for Model i |
| $\alpha_{in}^e$ | Fluid stiffness coefficients of n–th mode for Model i |
| $\xi$ | Dimensionless coordinates |
| $\zeta_n$ | Damping ratio in vacuum |
| $\gamma$ | Mass ratio (= $\rho\pi R^2/m$) |
| $\rho$ | Fluid density |
| $\omega_i$ | Circular frequency for Model i |
| $\omega_{in}$ | Natural frequency in radian of tube in vacuum |
| $\varphi_{in}(\xi)$ | Orthonormal function of n-th mode for Model i |

**Subscripts**

| | |
|---|---|
| i | i = 1, 2 for Model 1 and 2 |
| n | n-th modes |
| 1 | For Model 1 (TSP–inactive mode) |
| 2 | For Model 2 (TSP–active mode) |

# 1. INTRODUCTION

Extensive experimental and analytical studies have been performed on the dynamic response of loosely held tubes and how the tube response is related to wear (Chen, 1991 and Cai et al., 1991). Chen et al. (1984) investigated the fluidelastic behavior of loosely held tubes in the laboratory. They observed that, as the flow velocity is increased to a threshold value, or critical flow velocity, instability in the TSP-inactive mode may occur. Then, for a range of flow velocities higher than the threshold flow velocity, the tube vibrates predominantly in the TSP-inactive mode, with the response amplitude limited by the clearance between the tube and the TSP. With a further increase in flow velocity, a second threshold is reached and instability in the TSP-active mode begins. In this range, large-amplitude oscillations occur and, in many cases, tubes may impact one another. Additional experimental studies to determine the response of loosely supported tubes in the TSP-inactive mode under some specific flow conditions have recently been published (Nakamura and Fujita, 1987, Fisher and Ingham, 1988, Antunes et al., 1991).

In analyzing tube responses and impacting behavior of loosely supported tubes, many nonlinear methods have been developed in recent years. Numerical simulations were performed by Axisa et al. (1988), Fricker (1988) and Rao et al. (1988); all used quasistatic or quasisteady-flow theories, which are applicable in specific parameter ranges. Chen and Chandra (1990) developed the unsteady-flow model on fluidelastic instability of tubes in nonuniform flow. Cai et al (1991) presented a bilinear model, based on the unsteady-flow theory. The simulations by Cai et al. (1991) agreed reasonably well with the experimental data of Chen et al. (1984) and demonstrated that the unsteady-flow theory and the bilinear model are adequate to describe the nonlinear behavior of fluidelastic instability associated with TSP-inactive modes of loosely supported tubes in crossflow.

With the recent interest in chaotic motions of nonlinear systems (Moon, 1987) and the relationship of chaotic vibration to tube wear, it is appropriate to look into the possible existence of chaos in tube arrays in crossflow. Related system without flow have been studied experimentally by several investigators. Moon (1983), Shaw and Holmes (1983) and Shaw (1985a, 1985b) studied forced oscillation of beams with motion constraints; chaos was found to exist. A case study of chaos in a marine application, involving impacting modeled via bilinear springs was discussed by Thompson and Stewart (1986). Recently, it was realized that flow-induced vibration of loosely supported tubes, which is one of the systems with motion constraints, can display a wide variety of dynamic behavior. For example, chaotic fluidelastic vibrations of a constrained pipe conveying fluid were examined by Paidoussis and Moon (1988 and 1989) both experimentally and theoretically, with the use of a two-degree-of-freedom system. A study on chaotic and periodic motions of a nonlinear oscillator in order to model flow-induced vibration of loosely supported tubes was conducted by Langre et al. (1990).

Based on the unsteady-flow theory and the bilinear model, An analytical study on the dynamics of loosely supported tubes in crossflow has been performed (Cai and Chen, 1991). Many computations were conducted to confirm the existence of chaotic motion and the route to chaos with the change of control parameters in the instability region of the TSP-inactive mode. Indeed, chaotic motion was demonstrated as possible for such an autonomous system when several effective techniques, including bifurcation diagrams, phase flow portraits, power spectral density and Poincaré maps, were utilized in that study. Also, a preliminary test was conducted to obtain a convincing evidence of periodic/chaotic dynamics. The results of test are qualitatively in agreement with the analytical results based on the response spectral densities and observation.

The purpose of this paper is to apply the mathematical models and other techniques used in previous work of authors (Cai et al., 1991 and Cai and Chen, 1991), to extensively analyze the periodic/chaotic dynamics of the tube with nonlinear support in crossflow. The interesting regions of periodic and chaotic motion were expanded to the whole region of fluidelastic instability of tubes which associated with velocity-controlled negative damping between two threshold values of flow velocity. A route of chaotic-periodic-chaotic motions was predicted when values of negative damping varies with mean flow velocity in this region. Some new measure tools, like Lyapunov exponent and fractal dimension, were added in addition to others such as, phase portrait, power spectral density, and Poincaré map, for distinguishing the periodic/chaotic motions. Indeed, those measure tools were proved to be quite effective in predictions of existence of periodic and chaotic motion in the instability region. The tube response characteristics with various symmetric or asymmetric gaps are also studied. It is noted that nonlinearity of those symmetric or asymmetric gaps significantly affect the distributions of periodic, quasiperiodic and chaotic motions of the tube with various flow velocity in the instability region of the TSP-inactive mode.

## 2. EQUATIONS OF MOTION

An unsteady-flow theory for fluidelastic instability of a row of tubes in crossflow has been described in detail by Chen (1983, 1989) and by Chen and Chandra (1990). A bilinear mathematical model for loosely supported tubes vibrating in crossflow has been well defined by Cai et al (1991). For completeness, the unsteady flow model for fluidelastic instability of loosely supported tubes is briefly described here. The readers who are interested in further details of those theories can refer to our previous work.

Consider the case of fluidelastic instability in which a velocity-controlled negative damping mechanism is dominant. The stability of the tube row may be analyzed approximately by considering only one flexible tube among other rigid tubes and neglecting the coupling in the two directions. Therefore, a two-span flexible tube with one intermediate support, vibrating in one direction, is schematically shown in Figure 1. When the right end (C3) of the tube does not strike the stop, it is a pinned-pinned-free model (Model 1). When the right end strikes the stop, it becomes a pinned-pinned-spring-supported model (Model 2). Because the effects of impact force are represented by the linear springs at C3 in Model 2, the vibratory system is autonomous. Gaps $e_1$ and $e_2$ at C3 provide a nonlinear support for the system, which may cause the possible chaotic vibrations when some of system parameters vary in certain ranges.

The solutions of tube vibration by the normal-mode method can be described as two models analyzed in two different time regions (Cai et al., 1991)

$$\left.\begin{aligned} u(\xi,t) &= \sum_{n=1}^{\infty} a_{1n}(t)\phi_{1n}(\xi) \\ \dot{u}(\xi,t) &= \sum_{n=1}^{\infty} \dot{a}_{1n}(t)\phi_{1n}(\xi) \end{aligned}\right\} \quad 0 < t < t_s \qquad \text{(Model 1)} \qquad (1)$$

and

$$\left.\begin{aligned} u(\xi,t) &= \sum_{n=1}^{\infty} a_{2n}(t)\phi_{2n}(\xi) + u(\xi,t)\Big|_{t=t_s} \\ \dot{u}(\xi,t) &= \sum_{n=1}^{\infty} \dot{a}_{2n}(t)\phi_{2n}(\xi) \end{aligned}\right\} \quad t_s < t < t_d \qquad \text{(Model 2)} \qquad (2)$$

where $u(\xi,t)$ and $\dot{u}(\xi,t)$ are tube displacement and velocity; $\phi_{1n}(\xi)$ and $\phi_{2n}(\xi)$ are the normal modes of Models 1 and 2 (see Cai, et al., 1991); $\xi = z/\ell$; $t_s$ is the time that the right end of the tube strikes the stop, and $t_d$ is the time the tube end leaves the stop. $a_{1n}(t)$ and $a_{2n}(t)$ are the solutions of following equations

$$(1+\gamma\alpha_{in})\frac{da_{in}^2}{dt^2}+\left(2\zeta_n\omega_{in}-\frac{\gamma U_r^2}{\pi^3}\omega_i\alpha_{in}^d\right)\frac{da_{in}}{dt}+\left(\omega_{in}^2-\frac{\gamma U_r^2}{\pi^3}\alpha_{in}^e\right)a_{in}=0 \tag{3}$$

i = 1, 2 for Models 1 and 2

n = 1, 2, 3, ... $\infty$

where

$$\gamma=\frac{\rho\pi R^2}{m} \tag{4}$$

$$U_r=\frac{\pi U_m}{\omega_i R} \tag{5}$$

and

$$\omega_i=\sqrt{\frac{\omega_{in}^2-\frac{\gamma U_r^2}{\pi^3}\alpha_{in}^e}{1+\gamma\alpha_{in}}} \tag{6}$$

Note that R is tube radius, $\rho$ is fluid damping, m is tube mass per unit length and $U_m$ is mean flow velocity; $\alpha_{in}$ , $\alpha_{in}^d$ and $\alpha_{in}^e$ are added-mass coefficients, fluid-damping coefficients and fluid-stiffness coefficients which are based on the

experimental data of Tanaka (1980) and have been compiled and evaluated by Chen and Chandra (1990).

## 3. NUMERICAL SIMULATIONS

Numerical simulations of loosely supported tube schematically shown in Figure 1 were carried out with the system parameters similar to those applied in previous work (Cai and Chen, 1991). The span between supports C1 and C2 is submerged in fluid but subjected to flow at the middle portion only. The tube in Figure 1 is brass, with a 1.59 cm outside diameter, 1.59 mm wall thickness, and 123.15 cm length. The modulus of elasticity E is $1.11 \times 10^{-6}$ kg/cm$^2$. The impact stiffness of springs at the TSP is assumed to be a constant value, namely, $K_c = 10^7$ N/m. Gaps $e_1$ and $e_2$ are variable control parameters in simulations, they will range from 0.127 to 2.54 mm.

The computations were carried out on a Sun workstation computer. Before simulations, the natural frequencies of the first 10 modes for both Models 1 and 2 were calculated. Fluid force coefficients $\alpha_{in}$ , $\alpha_{in}^{d}$ and $\alpha_{in}^{e}$ were calculated based on Tanaka's data (1980) for a tube row with the pitch-to-diameter ratio of 1.33. Based on the natural frequencies of the first ten modes of the two models, the time-integration steps required during simulations can be determined. As verified in the previous studies (Cai et al., 1991 and Cai and Chen, 1991), 10 modes (covering a frequency range of 0-1700 Hz) give sufficient accuracy for this case. Therefore, 10 modes were used throughout, and the time-integration step for 10 modes was taken to be $\Delta t = 0.0001$ s to ensure the accuracy of simulations. Furthermore, a double-precision has to be taken throughout in simulations. Numerical integrations were run for a relative long fixed time to ensure that transient effects have died out before the output are examined. In our case, at

least 100,000 points were calculated for time histories of tube motions; then, the first 4,000 points in time histories calculated were taken out to eliminate transient effects.

## 4. CHAOTIC MEASUREMENTS

As summarized in the previous study (Cai and Chen, 1991), when flow velocity, which has been chosen as the main control parameter, is lower than the critical flow velocity, the system damping is positive and tube motion is stable, When flow velocity exceeds the critical flow velocity, the tube loses its stability and begins self-excitation oscillations, corresponding to a Hopf bifurcation. If the tube impacts the TSP irregularly in the instability region, tube motion depends on flow velocity and other parameters and chaotic motion may occur. If the tube impacts the TSP regularly after flow velocity exceeds some value in the instability region, tube motion is almost independent of flow velocity and periodic oscillations will occur with a fixed amplitude equal to the diametral clearance.

In this study, the focus is on the instability region, and more measurement techniques were taken to distinguish periodic and chaotic vibration of the tube. Many computations were performed. In following only some typical results will be presented.

### 4.1. Phase flow portraits

First of all, the time histories of tube motion with symmetric clearance $e_1 = e_2 =$ 1.27 mm at the TSP were calculated and phase flow diagrams at different flow velocities corresponding to periodic and chaotic motions are shown in Figure 2. In these calculation, the transient has been eliminated for clarity; only the

dynamics of the "steady state" are shown. Because the tube support span (see Figure 1) is asymmetric and the system is considered as a multiple-degree-of-freedom system, 10 modes are utilized to obtain accurate simulations. In Figure 2a, the phase portrait at $\xi$ = 1.0 for $U_m$ = 2.1 m/s is not an ellipse (as is that calculated by a single-degree-of-freedom), but a complicated closed circle. At this flow velocity, the tube impacts the TSP twice each circle; it corresponds to periodic oscillations that repeat very well. As flow velocity decreases and the absolute value of negative damping decreases, the number of tube impacts is reduced and the impact period appears to be irregular. Then, phase portrait (Figure 2b, $U_m$ = 2.0 m/s) appears chaotic – a kind of limited-band chaos. These chaotic motions apparently depend on the number of impacts during certain cycles, while impacts depend on the flow velocity, initial conditions, and other parameters such as clearance and contact stiffness.

### 4.2. Power spectral density

Figure 3 shows power spectra of tube motions at different flow velocities. It is observed that the fundamental oscillation frequencies at different flow velocities are approximately the same, i.e., $f_1$ = 29.6 Hz for the system shown in Figure 1; therefore, a nondimensional frequency $f/f_1$ is adopted in Figure 3. Figure 3a shows the PSD of the displacement at $U_m$ = 2.1 m/s, which appears to be periodic with super harmonic components, $f/f_1$ = 1, 3, 5, .... This is caused by regular tube impacting. Figure 3b presents characteristics of limited-band chaos, the power spectrum is a continuous process, although the fundamental frequency and superharmonic frequencies are still discernible in this process.

### 4.3. Poincaré map

The Poincaré map is a powerful technique for distinguishing chaotic responses from periodic responses. The map represents a discretization of a continuous flow in the phase space of a dynamic system. For an autonomous system, one must choose some plane in the phase space, transverse to the flow, and then obtain a Poincaré section (Moon, 1987). Using the same technique to choose a plane in our previous study (Cai and Chen, 1991), we chose the triggering signal, say when $\dot{u}(1.0,t) = 0$ and $u(1.0,t) < 0$, at which point the values of $U(0.371,t)$ and $\dot{u}(0.371,t)$ would be saved (here $\xi = 0.371$ means the middle point in the first span of the tube between C1 and C2). Figure 4a and 4b show such Poincaré maps, corresponding to flow velocities $U_m = 2.1$ m/s and $U_m = 2.0$ m/s, respectively. Figure 4a presents a periodic motion for there is only a single point in the phase plane. However, Figure 4b is a limited-band chaotic with points scattered over a wide range. In this case, although the Poincaré section do not display artistic merits because there are a limited number of data points, they nevertheless do seem to have certain structure, and confirm the existence of chaotic motion in this flow velocity range.

### 4.4. Lyapunov exponent

Lyapunov exponents have been proven to be the most useful dynamical diagnostic to determine chaotic system quantitatively. Lyapunov exponents are the average exponential rates of divergence or convergence of near by orbits in phase space. This technique gives a quantitative measurement for the corresponding motions, for example, the motion is periodic or chaotic, if the exponent is negative, zero or positive, respectively. Any system containing at least one positive Lyapunov exponent is defined to be chaotic. We use the algorithms proposed by Wolf et al (1985) to determine the Lyapunov exponents from a time

series of tube motion. Figure 5a and 5b show these results of Lyapunov exponents at different flow velocities. In Figure 5a, with $U_m$ = 2.1 m/s, Lyapunov exponents are negative, corresponding to a periodic motion of the tube. In Figure 5b, with $U_m$ = 2.0 m/s, Lyapunov exponents are positive. It indicates a convincing evidence for existence of chaotic motion in this instability region of the TSP-inactive mode.

### 4.5. Fractal dimension

Fractal dimension is another criterion for predicting chaotic motion quantitatively. A noninteger fractal dimension of the orbit in phase space implies the existence of a strange attractor. The basic idea is to characterize the "strangeness" of the chaotic attractor. The practical use of the fractal dimensions in measuring and characterizing chaotic vibrations has yet to be fully settled; different definitions have been developed including capacity dimension, correlation dimension and information dimension (Baker and Gollub, 1990). In many cases, it is sufficient to establish that the dimension is not integer or that the attractor is indeed strange. To the authors' best knowledge, this is the first application of the attractor dimension on fluidelastic instability of loosely supported tube in crossflow.

There are several methods to estimate the attractor dimensions. We use the measurement of correlation dimension which has been used successfully by many investigators in other fields (Moon, 1985). An extensive study of this definition of dimension has been given by Grassberger and Proccacia (1983). In this method, a correlation function C(r) can be calculated by constructing a sphere or length r at each point $x_i$ in phase space and counting the number of points in each sphere; that is

$$C(r) = \lim_{N\to\infty} \frac{1}{N^2} \sum_{\substack{i \\ i\neq j}}^{N} \sum_{j}^{N} H\left(r - \left|x_i - x_j\right|\right) \tag{7}$$

where H(s) = 1 if s > 0 and H(s) = 0 if s < 0. For many attractors this function has been found to exhibit a power law dependance on r as r → 0; that is

$$\lim_{r\to\infty} C(r) = a r^d \tag{8}$$

So that we may define a fractal or correlation dimension using the slope of log C versus log r curve:

$$d_G = \lim_{r\to\infty} \frac{\log C(r)}{\log r} \tag{9}$$

Using above technique, the correlation dimension of chaotic motion of the tube can be computed from the data of the Poincaré map in Figure 4b. Figure 6a shows the logarithm of the correlation function C(r) versus log r while Figure 6b shows the local slope of C(r). The slope for the intermediate values of r is around 1.6. This fractal dimension convinces that the attractor is indeed strange when the tube vibrating with this flow velocity range.

### 4.6. Bifurcation diagram

A widely used technique for examining the prechaotic or postchaotic changes in a dynamic system under parameter variations is the bifurcation diagram, from which we may find a route to chaos, namely a route from periodic to chaotic motions through parameter changes. With fast computers available, it is easy and helpful to vary the control parameters to obtain a bifurcation diagram. From this diagram, we can see if the system has steady or periodic or chaotic behavior

for some continuous range of flow velocity in order to obtain a full understanding of system dynamics. In this way, we can have confidence in deciding more definitely whether the system becomes chaotic. Also, we can observe and pinpoint sudden changes in system behavior. Both the control parameter and the output signal must be carefully chosen to ensure that they can provide sufficient information.

In our case, flow velocity was chosen as the control parameter and tube displacement as the output signal. The difficulty is in determining the locations of the triggering signal and output signal to produce an easily interpreted bifurcation diagram. On examining many results, the velocity of tube motion at location C3 ($\xi$ = 1.0) is taken as the triggering signal, and the displacement at location $\xi$ = 1.0 is taken as output signal. When the triggering signal is equal to zero, $\dot{u}(1.0,t) = 0$, and tube displacement at $\xi$ = 1.0 is negative, $u(1.0,t) < 0$, the values of u(1.0,t) are recorded. By slow variation of flow velocity, the bifurcation diagram is produced as shown in Figure 7, in which a symmetric clearance $e_1 = e_2$ = 1.27 mm at the TSP is applied.

It is clear in Figure 7 that for flow velocity less than the first critical flow velocity $U_m$ = 1.77 m/s or higher than the second critical flow velocity $U_m$ = 4.73 m/s (details see reference by Cai and Chen, 1991), all oscillations die out as time increases; when flow velocity reaches the critical values, there is a jump of displacement (i.e., the Hopf bifurcation occurs). When the tube loses its stability and the tube impacts the TSP, a chaotic motion occurs. But as flow velocity reaches certain values, between 2.02 m/s and 4.17 m/s, the tube impacts the TSP regularly in a harmonic periodic vibration due to the damping controlled instability of the tube. Therefore, the tube motion with above system parameters can be described as follow: first chaotic motion region ($U_m$ = 1.77 to 2.02 m/s), periodic motion region ($U_m$ = 2.02 to 4.17 m/s) and second chaotic motion region

($U_m$ = 4.17 to 4.77 m/s). This distribution of periodic/chaotic motions is correspondent to negative system damping. Figure 8 shows the negative damping as a function of flow velocity for Model 1. We note that when the absolute negative damping is below certain values, tube motion is chaotic, but when it exceeds those values it develop into periodic harmonic vibrations.

Many computations have been carried out for various diametral clearances at the TSP, symmetric or asymmetric, because we recognized that the nonlinearity of the TSP plays a very important role in periodic and chaotic motions of the tube. Bifurcation diagrams in Figure 9 give some results of these computations when asymmetric clearances were applied. In Figure 9, flow velocity changes from $U_m$ = 1.80 m/s to $U_m$ = 3.10 m/s, namely, from the first critical velocity to the flow velocity at which the absolute value of negative damping of Model 1 reaches maximum (see Figure 8). Also in Figure 9, we set $e_1$ always equal to 1.27 mm, but $e_2$ changed as 2.54, 1.45, 1.40 and 1.35 mm, corresponding to Figure 9a, 9b, 9c and 9d, respectively. The triggering signal and output signal are the same as those in Figure 7. From Figure 9, we noted that nonlinearity of those asymmetric gaps significantly affects the distributions of periodic and chaotic motions of the tube with various flow velocities in the instability region of the TSP-inactive mode. In Figure 9a, the tube does not strike the stop with the gap of $e_2$ anymore because $e_2$ = 2.54 mm almost likes an infinite gap under these system parameters. So, chaotic motion seems to be possible over almost whole range when flow velocity varies. When $e_2$ = 1.45 mm (Figure 9b), the tube begins to irregularly strike the stop with the gap of $e_2$ when flow velocity exceeds $U_m$ = 2.30 m/s. So there is another chaotic motion in this case. When $e_2$ = 1.40 mm and $e_2$ = 1.35 mm (Figure 9c and 9d), the tube begins to strike the stop regularly when flow velocities exceed some values, periodic and quasiperiodic motion are developing.

## 5. CONCLUSIONS

Based on the unsteady-flow theory and the bilinear mathematical model for fluidelastic instability of loosely supported tubes subjected to nonuniform crossflow, which were developed in our previous studies, an extensive analytical study has been conducted on the characteristics of fluidelastic instability of the tubes in the unstable region associated with the TSP-inactive mode, with particular attention given to the possible existence of chaotic oscillation. With a typical nonlinear boundary conditions, symmetric or asymmetric gaps at the TSP, tube motion can be expressed by a nonlinear autonomous mechanical system, in which a high probability of chaotic motion exists with variations of control parameters.

As suggested in most investigations on chaotic motions (Moon, 1987), it is important to use more than one measurement in deciding on the existence of chaos. Thus we carried out many measurements in this study, including phase flow portraits, power spectral density, Poincaré maps, Lyapunov exponents, fractal dimension and bifurcation diagram, to confirm the existence of chaotic motion in the instability region. Fortunately, measured results with those effective tools were in perfect agreement to convincingly demonstrate that at certain flow velocity range chaotic motions do arise. As shown in Figure 2 to 6, at flow velocity $U_m$ = 2.0 m/s, phase portrait displays a band circle to indicate a limited-band chaotic motion; PSD result presents a continuous limited-band spectrum; the Poincaré map gives a scattered structure; Lyapunov exponents appear to be a positive value; and fractal dimension is around 1.6 (not an integer). The importance of this, to our best knowledge, is that this is the first application of so many measurements which give consistent results in exploring the chaotic motion of loosely supported tubes that is induced by fluidelastic instability in crossflow.

The bifurcation diagrams show the route of chaotic-periodic-chaotic motions in the instability region corresponding to the variations of negative damping vs. the mean flow velocity. It is very important that the distribution of chaotic/periodic motions depends on the negative damping of both Models 1 and 2. When damping varies, the number of the tube impacts with the TSP will change. If the tube impacts the TSP regularly, it is periodic (or quasiperiodic) motion; if the tube impacts the TSP irregularly, chaotic motion may develop. This reminds us to pay more attention on impacting situation for predicting chaotic/periodic motions in further researches. Also, we note that nonlinearity of the TSP, with symmetric or asymmetric gaps, will significantly affect the distributions of periodic, quasiperiodic and chaotic motions of the tube with various flow velocity in the instability region of the TSP-inactive mode. Parameter analyses on chaotic motions will be continuously conducted to explore their behavior in more detail.

In this study a very complicated system, a tube with two asymmetric spans and subjected to nonuniform crossflow, was analyzed using 10 modes. Therefore, its chaotic behavior may be quite different to the systems with a single or two-degree-of-freedom as often investigated by many researchers to explore chaotic motions. Even though the analytical results in our studies indeed demonstrated existences and some characteristics of chaotic motion in the instability region of the TSP-inactive mode, we still have difficulties to completely understand many questions, like why does the chaotic motion occur and how can we control chaotic motion economically.

Obviously, further research on the chaotic motion on the fluidelastic instability of loosely supported tubes is still needed. A test, to obtain experimental data of periodic/chaotic motions for a loosely supported tube in crossflow, is being conducted at Argonne. Detailed comparison of the analytical and experimental

results will be published when it is completed. It will bring us more information and evidences of chaos on the fluidelastic instability of loosely supported tube in crossflow.

## ACKNOWLEDGMENTS

This work was sponsored by the U.S. Department of Energy, Office of Basic Energy Sciences, Division of Engineering and Geosciences.

## REFERENCES

Antunes, J., Axisa, F., and Vento, M. A., 1991, *Experiments on Vibro–Impact Dynamics Under Fluidelastic Instability,* ASME Pressure Vessels and Piping Conf., Nashville, TN, PVP Vol. 189, pp. 127–138.

Axisa, F., Antunes, J., and Villard, B., 1988, *Overview of Numerical Methods for Predicting Flow–Induced Vibration,* Trans. ASME Pressure Vessels and Piping, Vol. 110, pp. 6–14.

Baker, G. L., and Gollub, J. P., 1990, *Chaotic Dynamics,* New York: Cambridge University Press.

Cai, Y., and Chen, S. S., 1991, *Chaotic Dynamics of Loosely Supported Tubes in Crossflow,* Argonne National Laboratory Report ANL–91/30 (July 1991).

Cai. Y., Chen, S. S., and Chandra, S., 1991, *A Theory for Fluidelastic Instability of Tube–Support–Plate Inactive Modes,* ASME Pressure Vessels and Piping Conf., San Diego, CA, PVP–Vol. 206, pp. 9–18; To appear in Journal of Pressure Vessel Technology.

Chen, S. S., 1989, *Some Issues Concerning Fluidelastic Instability of a Group of Circular Cylinders in Cross–Flow,* Trans. ASME, J. Press. Vessel Technol., Vol. 111, pp. 507-518.

Chen, S. S., and Chandra, S., 1990, *Fluidelastic Instabilities in Tube Bundles Exposed to Nonuniform Crossflow,* ASME Pressure Vessels and Piping Conf., Nashville, TN, PVP Vol. 189, pp. 65–77.

Chen, S. S., 1991, *A Review of Dynamic Tube–Support Interaction in Heat Exchanger Tubes,* Presented at the Fifth International Conf. on Flow Induced Vibrations, Brighton, England, Paper C416/012.

Chen, S. S., Jendrzejczyk, J. A., and Wambsganss, M. W., 1984, *Dynamics of Tubes in Fluid with Tube–Baffle Interaction,* ASME Symp. on Flow–Induced Vibration, New Orleans, Vol. 2, pp. 285–304.

Chen, S. S., 1983, *Instability Mechanism and Stability Criteria of a Group of Circular Cylinders Subjected to Crossflow, Part 1: Theory,* J. Vibration, Acoustics, Stress and Reliability in Design, Vol 105, pp. 51–58.

Fisher, N. J., and Ingham, B., 1988, *Measurement of Tube–to–Support Dynamic Force in Fretting–Wear Rigs,* International Symp. on Flow–Induced Vibration and Noise, Chicago, Vol. 5, pp. 137–156.

Fricker, A. J., 1988, *Numerical Analysis of the Fluidelastic Vibration of a Steam Generator Tube with Loose Supports,* International Symp. on Flow–Induced Vibration and Noise, Chicago, Vol. 5, pp. 105–120.

Grassberger, P., and Proccacia, J., 1983, *Measuring the Strangeness of Strange Attractors,* Physica, Vol. 9D, 189–208.

Langre, E. de, et al., 1990, *Chaotic and Periodic Motion of a Non–Linear Oscillator in Relation with Flow–Induced Vibrations of Loosely Supported Tubes,* ASME Pressure Vessels and Piping Conf., Nashville, TN, PVP Vol. 189, pp. 119–125.

Moon, F. C., 1987, *Chaotic Vibrations,* New York: John Wiley.

Moon, F. C., and Shaw, S. W., 1983, *Chaotic Vibrations of a Beam with Non–Linear Boundary Conditions,* Int. J. Non–Linear Mechanics, Vol. 18, pp. 465–477.

Nakamura, T., and Fujita, K., 1987, *A Study on Impact Vibration of Loosely Held Tube by Cross Flow,* International Conf. on Flow Induced Vibrations, Bowness–on–Windermere, England, Paper K1, pp. 427–436.

Paidoussis, M. P., and Moon, F. C., 1988, *Nonlinear and Chaotic Fluidelastic Vibrations of a Flexible Pipe Conveying Fluid,* J. Fluids and Structures, Vol. 2, pp. 567–591.

Paidoussis, M. P., and Moon, F. C., 1989, *Chaotic Oscillations of the Autonomous System of a Constrained Pipe Conveying Fluid,* J. Sound Vib., Vol. 135(1), pp. 1–19.

Rao, M. S. M., Steininger, D. A., and Eisinger, F. L., 1988, *Numerical Simulation of Fluidelastic Vibration and Wear of Multispan Tubes with Clearances at Supports,* International Symp. on Flow–Induced Vibration and Noise, Chicago, Vol. 5, pp. 235–250.

Shaw, S. W., 1985a, *The Dynamics of a Harmonically Excited System Having Rigid Amplitude Constraints; Parts I and II,* ASME J. Appl. Mech., Vol. 52, pp. 453–458 and pp. 459–469.

Shaw, S. W., 1985b, *Forced Vibrations of a Beam with One–Sided Amplitude Constraint: Theory and Experiment,* J. Sound Vib., Vol. 99, pp. 199–212.

Shaw, S. W., and Holmes, P. J., 1983, *A Periodically Forced Piecewise Linear Oscillator,* J. Sound Vib., Vol. 90, pp. 129–155.

Tanaka, M., 1980, *Study on Fluidelastic Vibrations of Tube Bundle,* Jpn. Soc. Mech. Eng., Trans., Section B, Vol. 46(408), pp. 1398-1407.

Thompson, J. M. T., and Stewart, H. B., 1986, *Nonlinear Dynamics and Chaos,* New York: John Wiley.

Wolf, A., Swift, J. B., Swinney, H. L., and Vastano, J. A., 1985, *Determining Lyapunov Exponents from a Time Series,* Physics, Vol 16D, 285–317.

Fig. 1. Schematic of tube and supports in crossflow

Fig. 2. Phase flow portraits at $\xi = 1.0$ with (a) $U_m = 2.1$ m/s and (b) $U_m = 2.0$ m/s

Fig. 3. Power spectral density of tube displacement with (a) $U_m = 2.1$ m/s and (b) $U_m = 2.0$ m/s

Fig. 4. Poincaré map of tube motion at $\xi = 0.371$ with (a) $U_m = 2.1$ m/s and (b) $U_m = 2.0$ m/s

Fig. 5. Lyapunov exponents of tube motion with (a) $U_m = 2.1$ m/s and (b) $U_m = 2.0$ m/s. (Embedding dimension is selected to be 6 and delay time to be 1/2 of mean orbital period.)

Fig. 6. Correlation function (a) and correlation dimension (b) for the set of points in the Poincaré map in Fig. 4b

Fig. 7. Bifurcation diagram of tube motion in the instability region

Fig. 8. System damping ratio vs. mean flow velocity

Fig. 9. Bifurcation diagrams of tube motion with asymmetric clearances $e_1 = 1.27$ mm and (a) $e_2 = 2.54$ mm, (b) $e_2 = 1.45$ mm, (c) $e_2 = 1.40$ mm, and (d) $e_2 = 1.35$ mm

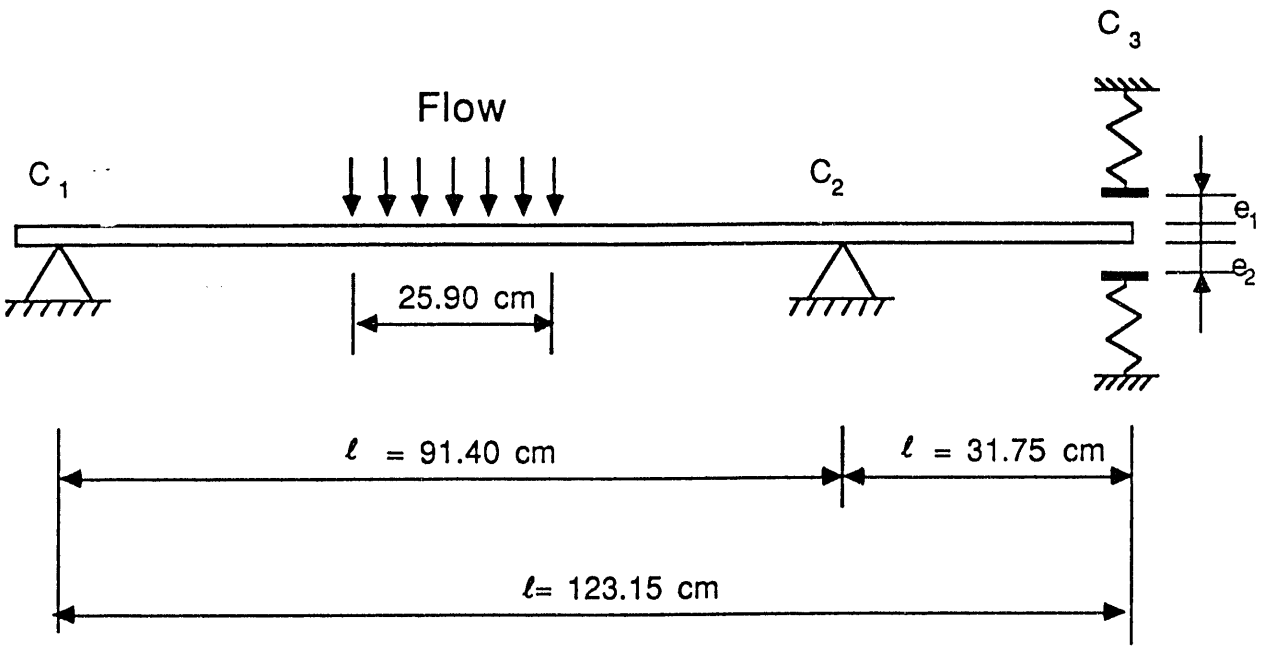


Fig. 1

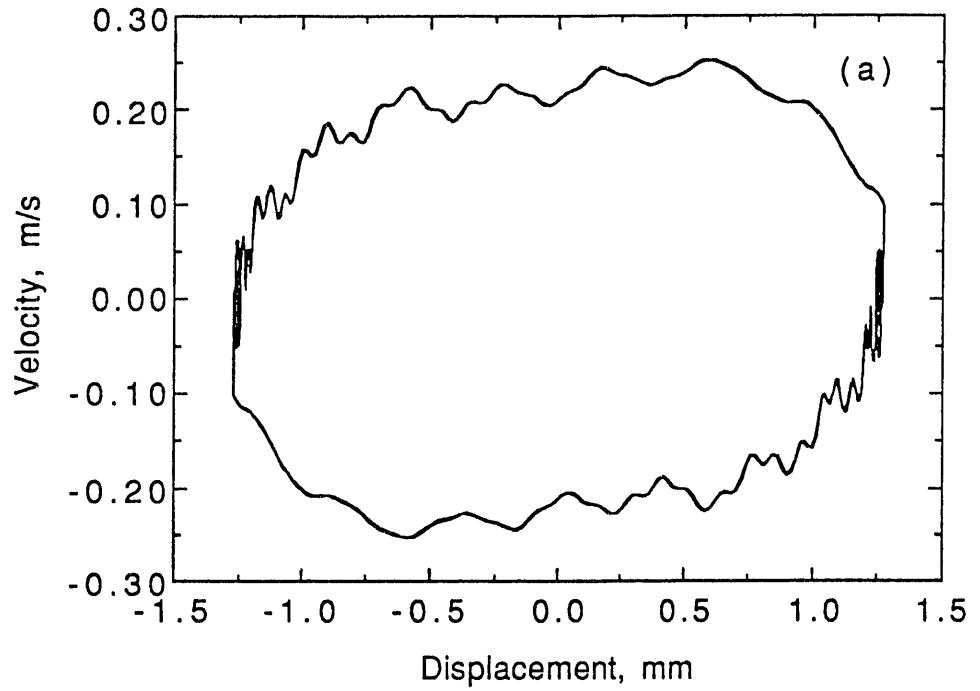
(a)
0.30
0.20
0.10
0.00
-0.10
-0.20
-0.30
Velocity, m/s
-1.5
-1.0
-0.5
0.0
0.5
1.0
1.5
Displacement, mm

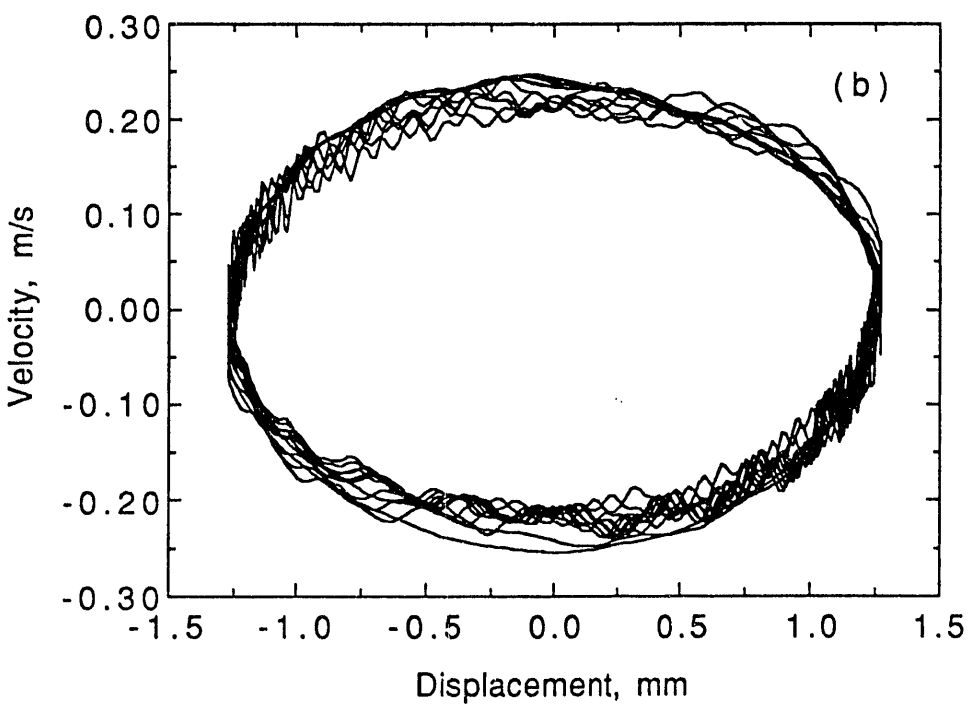
(b)
0.30
0.20
0.10
0.00
-0.10
-0.20
-0.30
Velocity, m/s
-1.5
-1.0
-0.5
0.0
0.5
1.0
1.5
Displacement, mm

Fig. 2

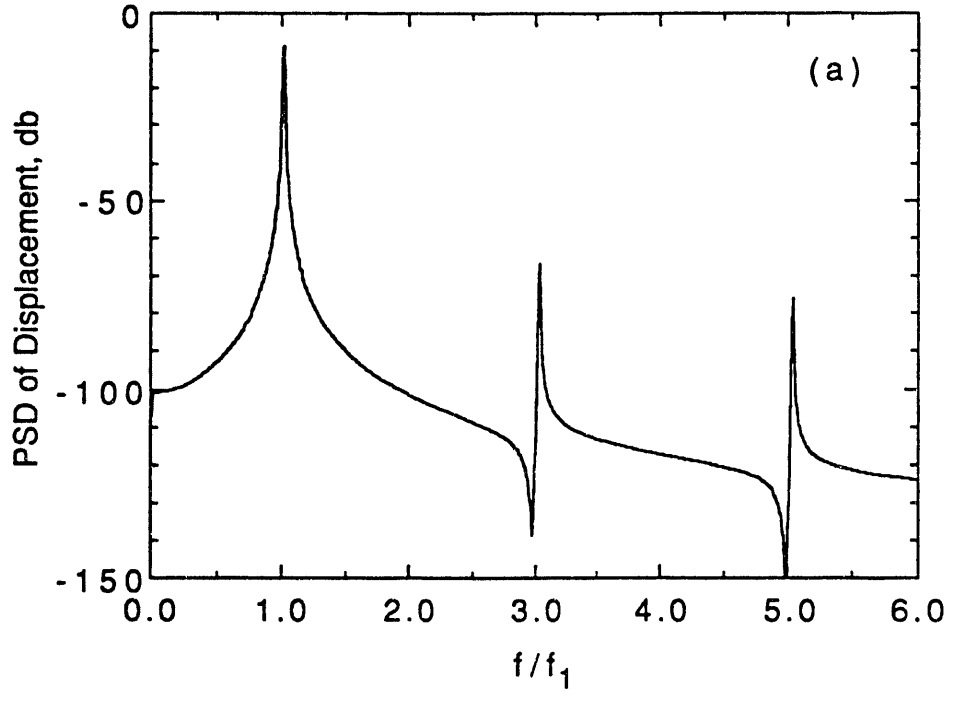
(a)
PSD of Displacement, db
0
-50
-100
-150
0.0
1.0
2.0
3.0
4.0
5.0
6.0
f/f1

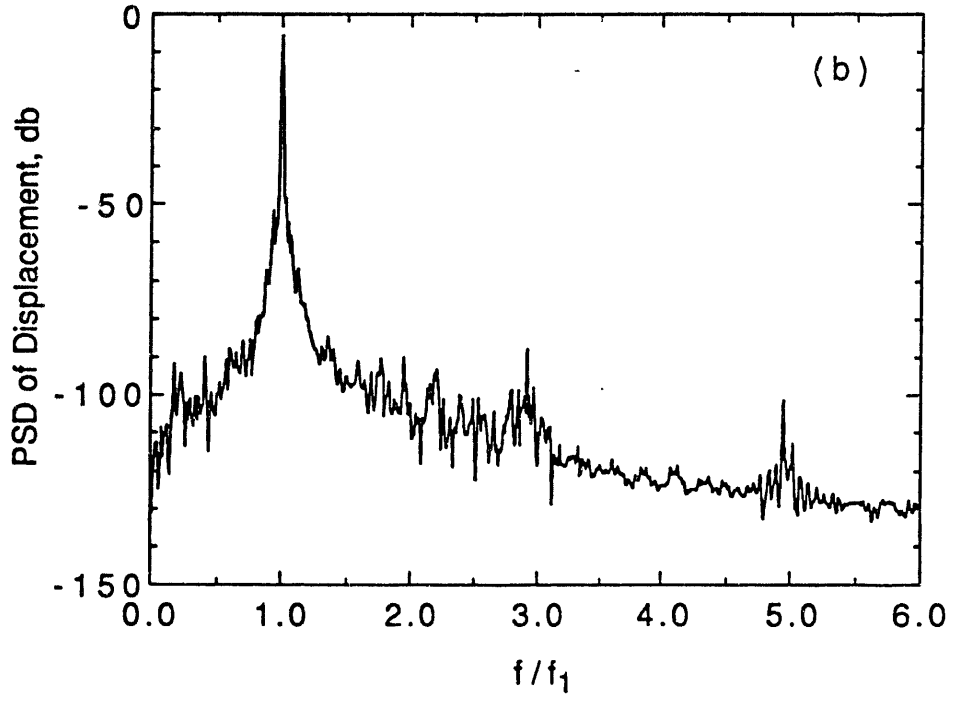
(b)
PSD of Displacement, db
0
-50
-100
-150
0.0
1.0
2.0
3.0
4.0
5.0
6.0
f/f1

Fig. 3

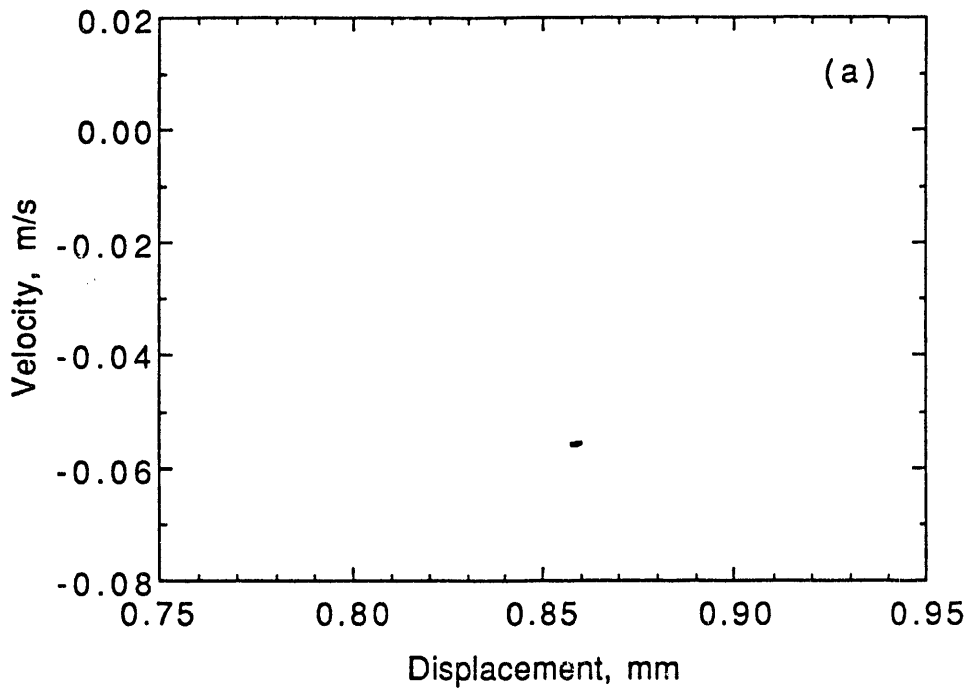
(a)
0.02
0.00
-0.02
-0.04
-0.06
-0.08
Velocity, m/s
0.75
0.80
0.85
0.90
0.95
Displacement, mm

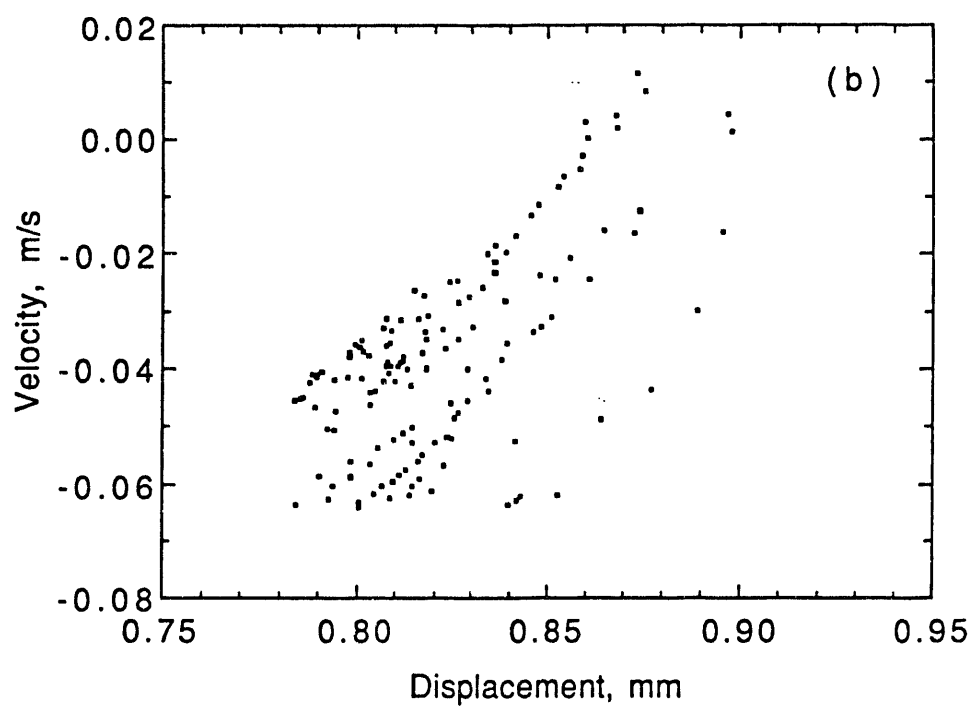
(b)
0.02
0.00
-0.02
-0.04
-0.06
-0.08
Velocity, m/s
0.75
0.80
0.85
0.90
0.95
Displacement, mm

Fig 4

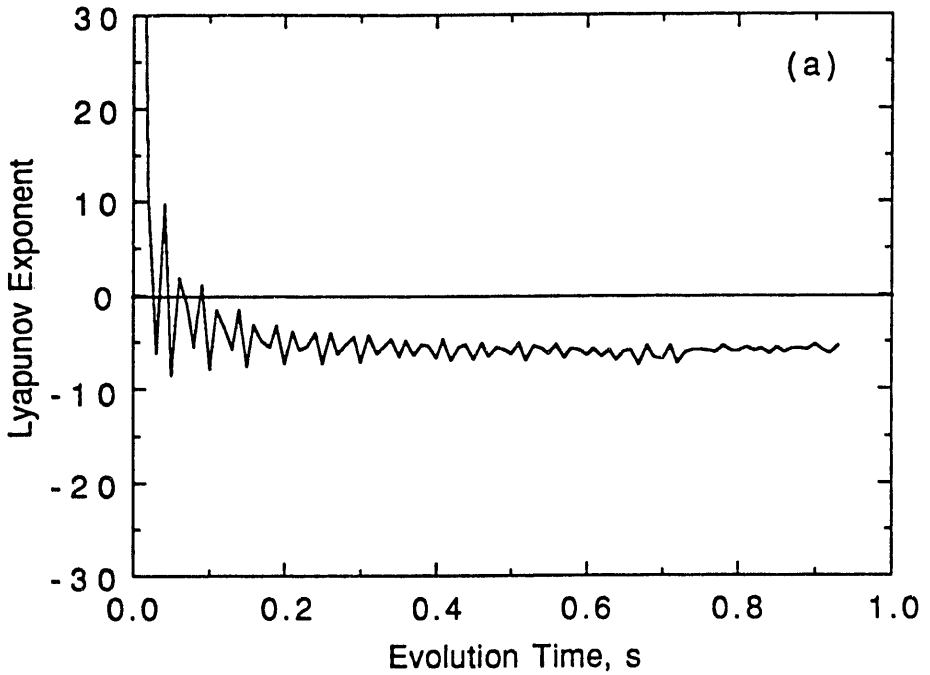
(a)
30
20
10
0
-10
-20
-30
Lyapunov Exponent
0.0
0.2
0.4
0.6
0.8
1.0
Evolution Time, s

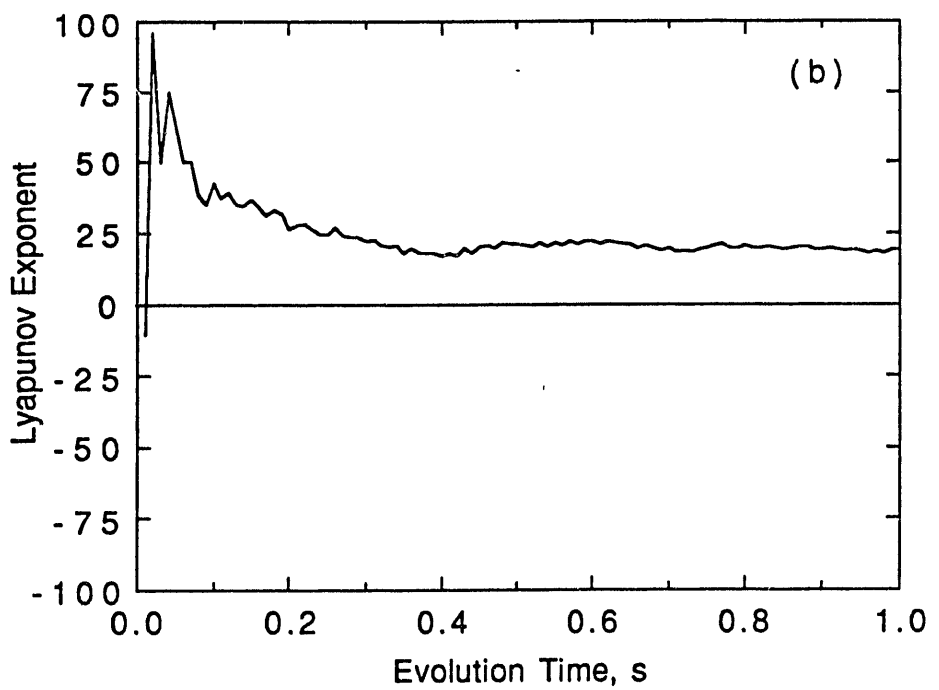
(b)
100
75
50
25
0
-25
-50
-75
-100
Lyapunov Exponent
0.0
0.2
0.4
0.6
0.8
1.0
Evolution Time, s

Fig. 5

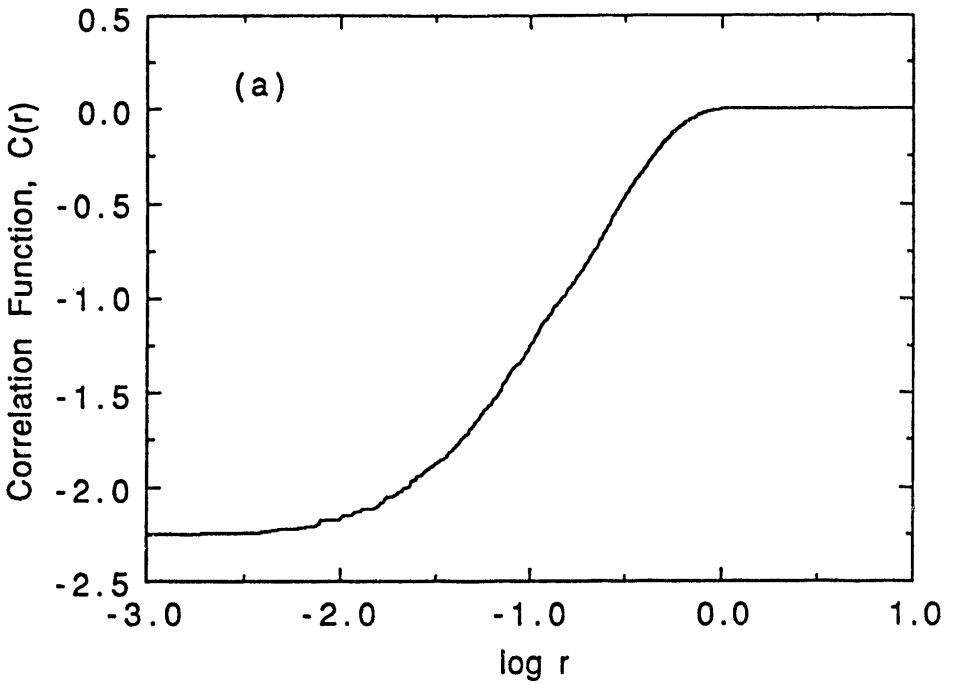
(a)
Correlation Function, C(r)
0.5
0.0
-0.5
-1.0
-1.5
-2.0
-2.5
-3.0
-2.0
-1.0
0.0
1.0
log r

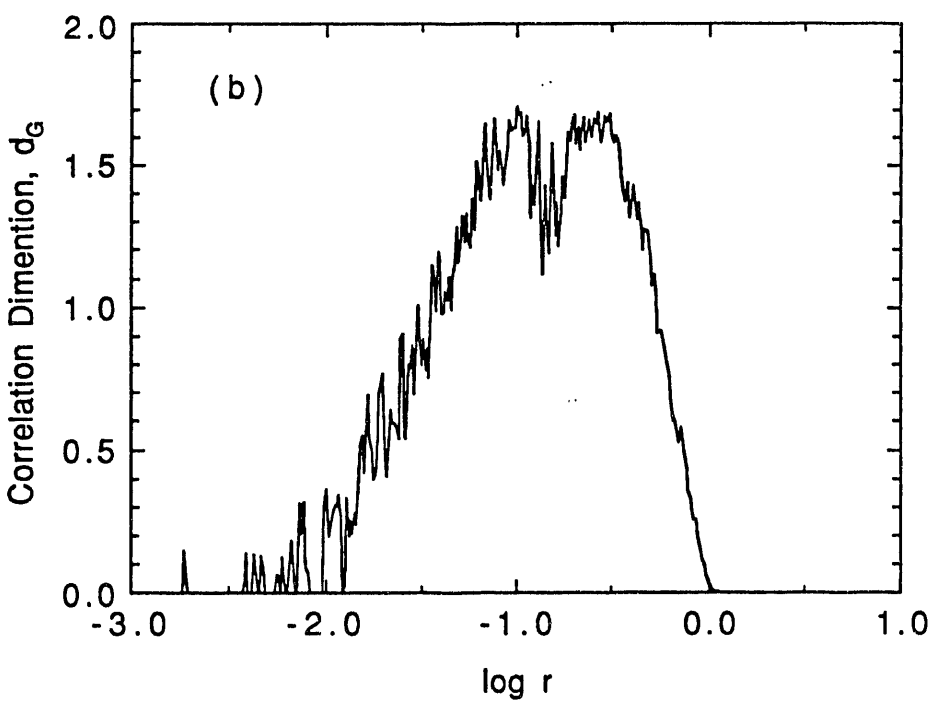
(b)
Correlation Dimention, $d_G$
2.0
1.5
1.0
0.5
0.0
-3.0
-2.0
-1.0
0.0
1.0
log r

Fig. 6

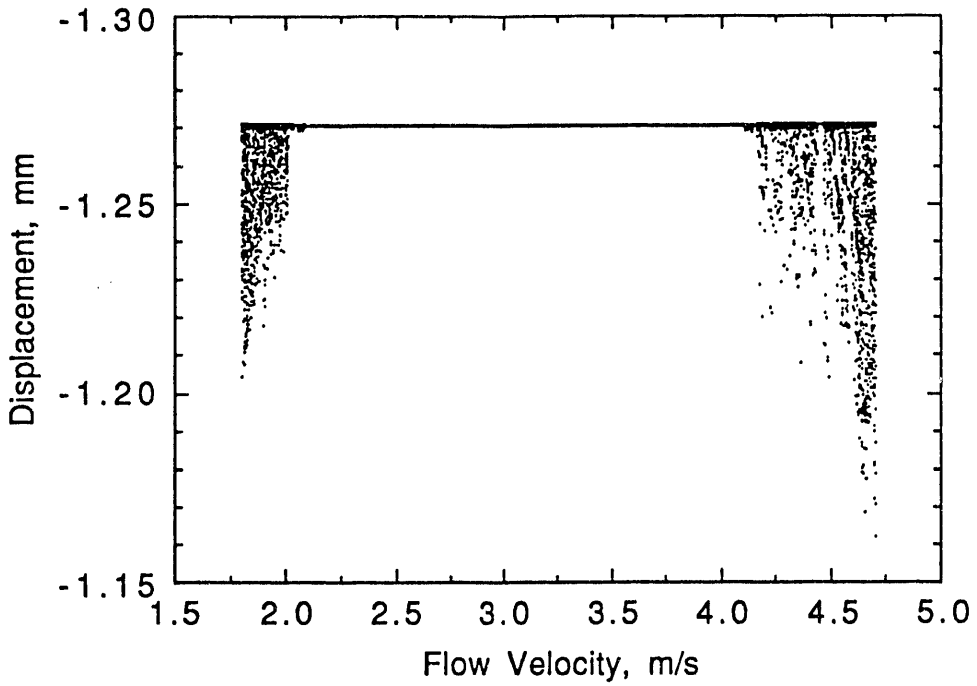
-1.30
-1.25
-1.20
-1.15
Displacement, mm
1.5
2.0
2.5
3.0
3.5
4.0
4.5
5.0
Flow Velocity, m/s

Fig. 7

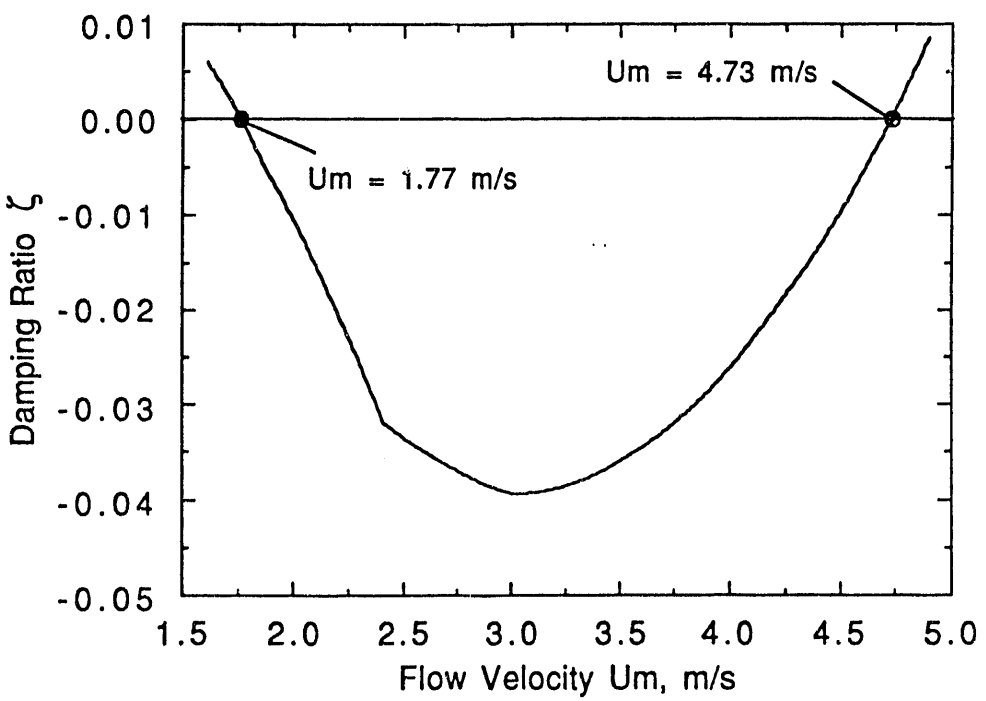
0.01
0.00
-0.01
-0.02
-0.03
-0.04
-0.05
Damping Ratio ζ
Um = 4.73 m/s
Um = 1.77 m/s
1.5
2.0
2.5
3.0
3.5
4.0
4.5
5.0
Flow Velocity Um, m/s

Fig. 8

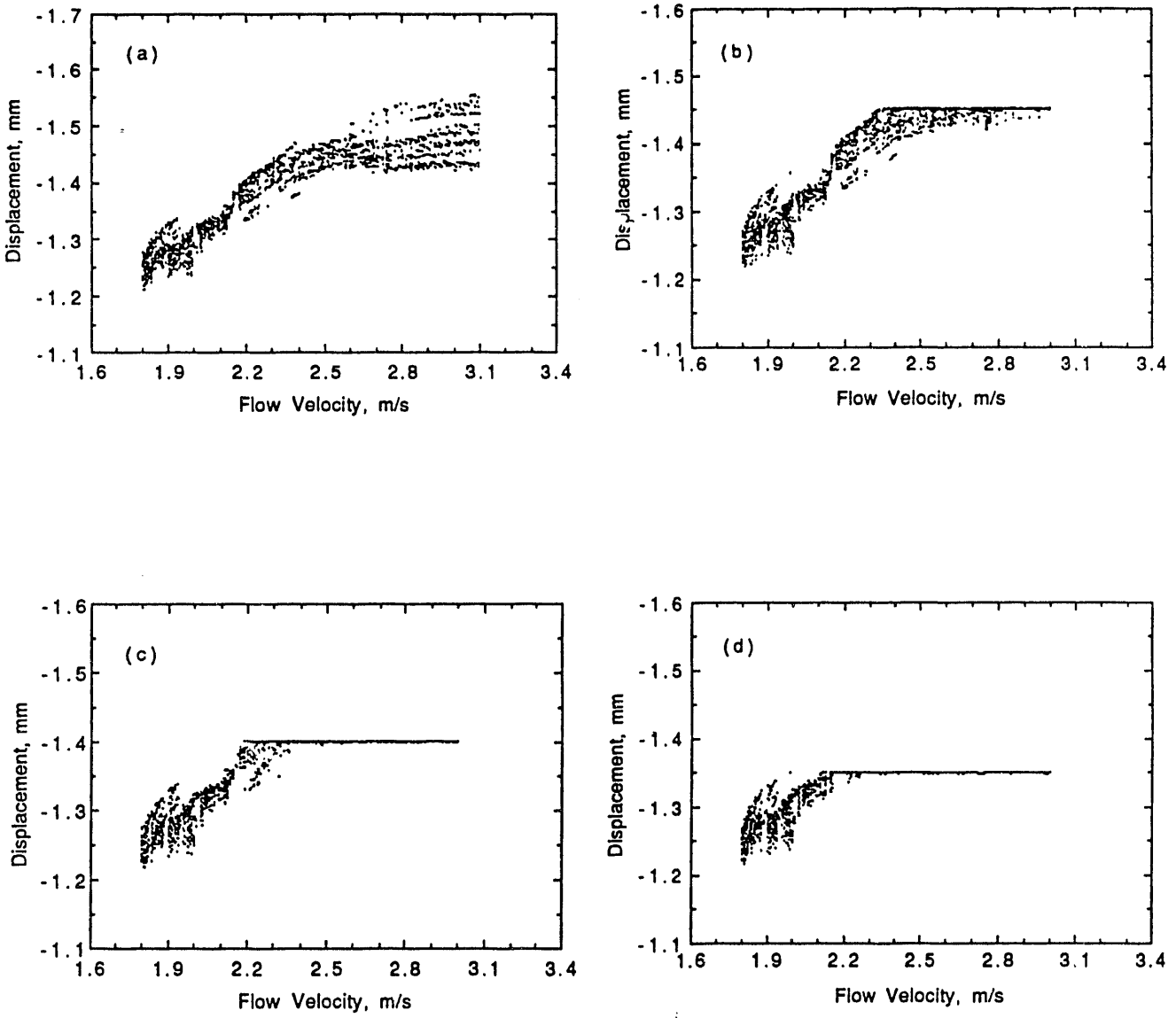
(a)
(b)
(c)
(d)
Displacement, mm
Flow Velocity, m/s
-1.7
-1.6
-1.5
-1.4
-1.3
-1.2
-1.1
1.6
1.9
2.2
2.5
2.8
3.1
3.4

Fig. 9

# END

# DATE FILMED

2/19/93